FLUID-STRUCTURE COUPLING RESEARCH FOR MICRO FLAPPING-WING

Yang WenQing, Song BiFeng, Song WenPing, Li ZhanKe
School of Aeronautics, Northwestern Polytechnical University, Xi'an, P.R. China, 710072

Keywords: *flapping wing; fluid-structure coupling; RANS equations*

Abstract

A method of fluid-structure coupling research for micro flapping wing is presented in this paper. The wings of FMAV (Flapping-wing Micro Air Vehicle) always are light weight and elastic structure. The wings will deform by the pressure of aerodynamic force generated by the flapping motion. The fluid-structure coupling problem is important to study the true state of flapping wing.

The aerodynamic forces are obtained by solving the RANS (Reynolds-Averaged Navier-Stokes) equations. The preconditioning method is used to solve the convergence problem in low speed. The chimera grids method is used to simulate the flapping wing.

The stiffness matrix used in computational structure deformation is tested by experiment in high precision. An experiment method based on linear fitting is developed to test the stiffness matrix of flexible wing. The distributing surface forces are translated onto the structure nodes. The motion governing equations are simplified for preliminary research. Inertial force and damping force are ignored because the flapping frequency is far less than the natural frequency. The method is the basic trial to study the effect of elastic deformation of flexible flapping wing to the aerodynamic characteristics.

The results show that the deformation of flexible wing will decrease the fluctuation of aerodynamic forces generated by wings' flapping motion. The deformation is generated mainly by lift, and the average lift will decrease a little but the thrust will increase for the deformation manner of relatively rigid leading edge. Therefore proper flexible wing will increase the thrust and make the air vehicle more stable.

1 Introduction

Flapping wings can generate lift and thrust simultaneously. Flapping-wing Micro Air Vehicle (FMAV) is a kind of new conception bionic air vehicle. Many researchers have done much study on FMAV by theoretical, experimental and numerical methods. And many productions have been got by the numerical method in simulating the flow field of FMAV by Computational Fluid Dynamic (CFD) [1-5].

Most of researches are concern about the given moving law and corresponding aerodynamic force. However, the wings of FMAV are always light and elastic, and they will deform under the pressure of aerodynamic force. The aerodynamic performance will change with wing deformation. Then the aerodynamic force and the structure deformation is a loop interaction. Hence, it is necessary to analyze the interaction effect between structure deformation and aerodynamic forces. This is helpful to confirm the true state of flexible flapping wing.

This paper presents a fluid-structure coupling method to study the effect of structure deformation on the aerodynamic performance of micro flapping-wing.

The aerodynamic forces are obtained by solving the preconditioned RANS equations. And the stiffness matrix is tested by experiment in high precision. The inertial force and damping force are ignored because the wings

* Supported by the National Science Foundation of China (Grant No. 10802066)

are light weight, elastic structure and flapping frequency is far less than the natural frequency.

2 Motion Governing Equation

Based on the Rayleigh-Ritz method, the governing equation of motion [6] is,

$$\mathbf{M}\ddot{\mathbf{q}}(t)+\mathbf{D}\dot{\mathbf{q}}(t)+\mathbf{K}\mathbf{q}(t)=\mathbf{F}(t) \qquad (1)$$

where $\mathbf{M}$, $\mathbf{D}$, $\mathbf{K}$ are mass, damping, stiffness matrices, respectively. They are independent on the fluid, but dependent on the wing structure and time. $\mathbf{q}(t)$ is structure displacement vector. $\mathbf{F}(t)$ is aerodynamic force vector.

For linear hypotheses, the mass, damping, stiffness matrices are independent on time, then the structure parameters are independent on the aerodynamic forces. The mass, damping, stiffness matrices are considered to be constant.

The motion of flapping wing is driven by the flapping organ, and the flapping motion generates the aerodynamic forces, but the aerodynamic forces depress the flexible wings and make them deform. Therefore the flapping frequency is equal to the frequency of variety of aerodynamic forces. The aerodynamic forces caused by flapping motion are the input cause. The deformation of wings caused by the aerodynamic forces is the unknown output result need to be solved. The problem is that the output and input are loop interaction.

Based on the vibration theory [7], there is a relationship between the aerodynamic force frequency ω and the natural structure frequency ω_n Let $\lambda=\omega/\omega_n$ be frequency ratio. The natural structure frequency of the wings in this paper is about 20Hz, but the aerodynamic force frequency is 3-6Hz which is equal to the flapping frequency. Therefore, $\lambda \ll 1$, the elastic force $\mathbf{K}\mathbf{q}(t)$ is the dominating force, so the inertial force $\mathbf{M}\ddot{\mathbf{q}}(t)$ and damping forces $\mathbf{D}\dot{\mathbf{q}}(t)$ can be ignored. Then, Eq.(1) changes to,

$$\mathbf{K}\mathbf{q}(t)=\mathbf{F}(t) \qquad (2)$$

Eq.(2) can be expressed as,

$$\mathbf{K}^{-1}\mathbf{F}(t)=\mathbf{q}(t) \qquad (3)$$

$\mathbf{K}^{-1}$ is tested by experiment in high precision, $\mathbf{q}(t)$ can be calculated by Eq.(3) after $\mathbf{F}(t)$ is obtained.

Eq.(3) is a simplified equation because the inertial and damping forces are ignored. For the basic research, this is a reasonable simplification.

3 Structure Stiffness Matrix Experiment

The wing structure is shown in Fig.1. The leading edge and wing ribs are made of carbon fiber and the wing skin is anti-puncture polyester membrane. The membrane can just support tension, so the carbon fiber framework supports the main deformation. The structure nodes are chosen as Fig.1. The displacement vertical to wing surface is dominating, and displacements in other directions are ignored.

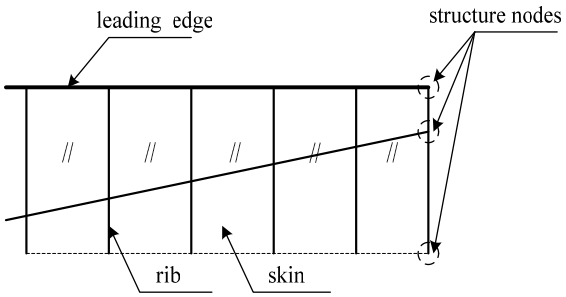

Fig.1 structure nodes of flapping wing

Each wing has N structure nodes, so $\mathbf{K}$ and $\mathbf{K}^{-1}$ are matrices with dimension of $N\times N$, $\mathbf{q}(t)$ and $\mathbf{F}(t)$ are vectors of $N\times 1$. N=15 for the wing in Fig.1. $\mathbf{K}^{-1}$ is tested by experiment method. If only put a unit force on the jth node vertical to wing surface, the force vector is,

$$\mathbf{F}_j(t)=(\underbrace{0,...,0}_{j-1},1,\underbrace{0,...,0}_{N-j})^T \qquad (4)$$

Then test the displacement of all structure nodes, and get the displacement vector,

$$\mathbf{q}_j(t)=(q_{1,j},...,q_{i-1,j},q_{i,j},q_{i+1,j},...,q_{N,j})^T \qquad (5)$$

Now, Eq.(3) becomes,

$$\mathbf{K}^{-1}\mathbf{F}(t) = \left(k_{1,j}^{-1},\cdots,k_{i-1,j}^{-1},k_{i,j}^{-1},k_{i+1,j}^{-1},\cdots,k_{N,j}^{-1}\right)^T = \left(q_{1,j},\cdots,q_{i-1,j},q_{i,j},q_{i+1,j},\cdots,q_{N,j}\right)^T \quad (6)$$

According to Eq.(3)-(6), Eq.(7) can be derived,

$$k_{i,j}^{-1} = q_{i,j} \quad (7)$$

Put unit force to all the structure nodes, we can get the total $\mathbf{K}^{-1}$.

In order to test the stiffness matrix in high precision, a method is developed based on the linear fitting. The basic manner is putting a series of forces onto every structure node and testing the displacement of all structure nodes. Based on Eq.(3) the displacement is linear with the forces. Because the results of experiments have error, the slope of line with linear fitting is chosen to be the test results which have little error. The method can also examine the linearity between displacements and forces. The displacement is obtained by the laser ranging shown in Fig.2.

Fig.2 KEYENCE laser ranging device

The nodes number is shown in Fig.3. The wing root is together with the flapping organ, so their deformation displacements are zero.

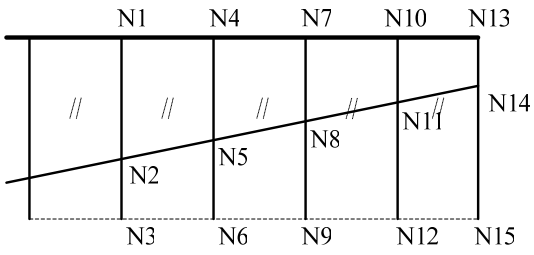

Fig.3 nodes number

Test results are shown in Fig.4 and Fig.5. Fig.4 shows the linearity between displacements and forces. Fig.5 shows the results of wing displacements.

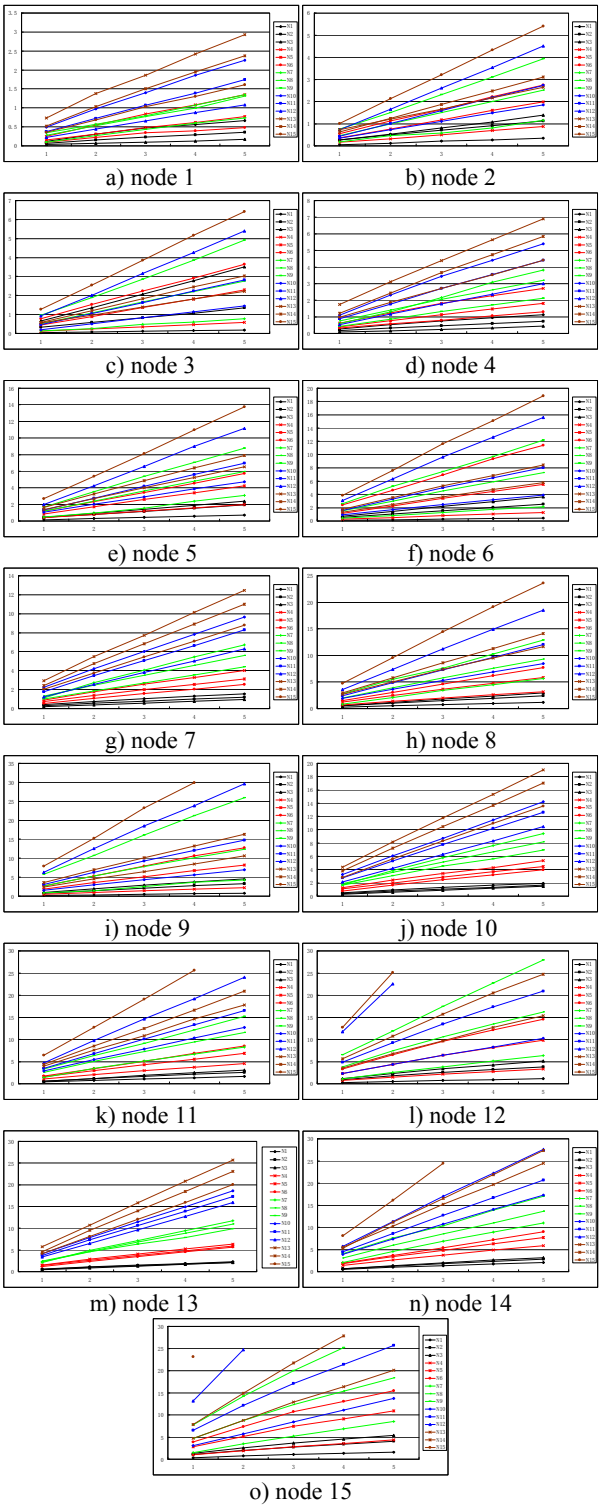

Fig.4 linearity between displacements and forces when putting forces to every node (the lateral axis is the force in '×10g', the vertical axis is the deformation displacement in 'mm')

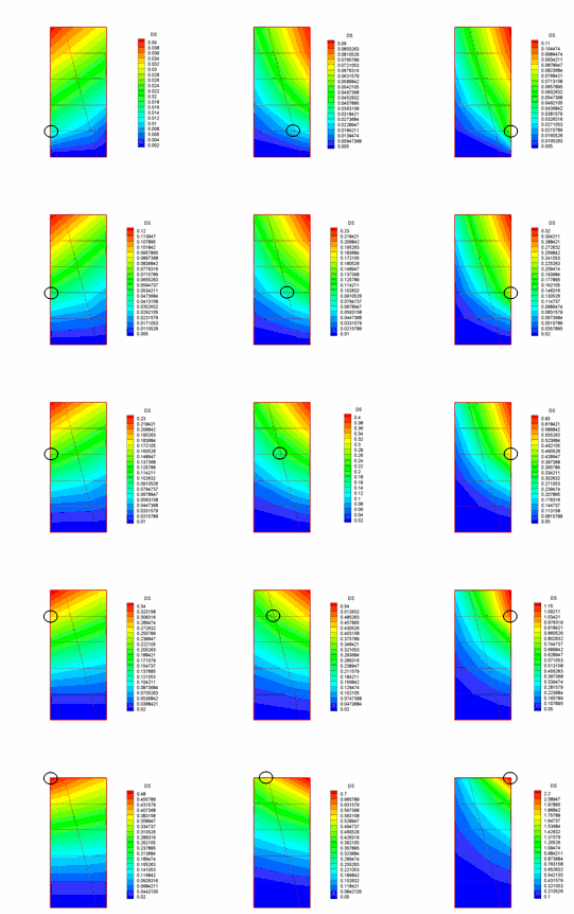

Fig.5 displacement of wing (the left edge is leading edge, the bottom edge is the wing root, the leading edge is stiffer and deform less)

Using the tested value to examine the fitting value, the average error is 2.65%. The results can demonstrate the method has high precision.

4 Numerical Method

The numerical method is based on preconditioned Reynold-Averaged Navier-Stokes equations [8],

$$\boldsymbol{\Gamma}^{-1}\frac{\partial \mathbf{W}_T}{\partial \tau}+\frac{\partial \mathbf{W}}{\partial t}+\frac{\partial(\mathbf{E}-\mathbf{E}_v)}{\partial x}+\frac{\partial(\mathbf{F}-\mathbf{F}_v)}{\partial y}+\frac{\partial(\mathbf{G}-\mathbf{G}_v)}{\partial z}=0 \qquad (8)$$

$$\mathbf{W}_T=[\rho,u,v,w,T]^{\mathrm{T}}$$
$$\mathbf{W}=[\rho,\rho u,\rho v,\rho w,\rho E]^{\mathrm{T}}$$
$$\mathbf{E}=[\rho u,\rho u^2+p,\rho uv,\rho uw,\rho Hu]^{\mathrm{T}}$$
$$\mathbf{F}=[\rho v,\rho uv,\rho v^2+p,\rho vw,\rho Hv]^{\mathrm{T}}$$
$$\mathbf{G}=[\rho w,\rho wu,\rho wv,\rho w^2+p,\rho Hw]^{\mathrm{T}}$$
$$\mathbf{E}_v=[0,\sigma_{xx},\sigma_{xy},\sigma_{xz},\beta_x]^{\mathrm{T}}$$
$$\mathbf{F}_v=[0,\sigma_{yx},\sigma_{yy},\sigma_{yz},\beta_y]^{\mathrm{T}}$$
$$\mathbf{G}_v=[0,\sigma_{zx},\sigma_{zy},\sigma_{zz},\beta_z]^{\mathrm{T}}$$

Here, $\boldsymbol{\Gamma}^{-1}$ is preconditioning matrix, the τ is pseudo time, the t is true time, $\mathbf{E}$, $\mathbf{F}$, $\mathbf{G}$ are inviscous flux, and $\mathbf{E}_v$, $\mathbf{F}_v$, $\mathbf{G}_v$ are viscous flux. ρ, (u,v,w), p, E, H are density of fluid, the three direction velocities in Cartesian coordination, pressure, total energy, total enthalpy. σ_{**}, β_* are viscous stress and heat transfer.

The spatial discretization is characterized by a second-order cell-center method for finite volumes. A five-stage Runge-Kutta scheme is employed to achieve convergence of the solution by integration with respect to time. For unsteady flows an implicit dual time-stepping scheme is used. Implicit residual smoothing is employed to accelerate convergence. The Spalart-Allmaras turbulent model is applied for calculating the turbulence flows.

The grid system of flapping wing is based on the chimera grids method. In chimera method, the trilinear interpolation is used in the grid interface communication. More details are in reference [9].

The true wing is thin and the muller thin plate airfoil [10] is chosen. The airfoil thickness is 1.96%, shown in Fig.6. Wing grid is shown in Fig.7.

Fig.6 muller airfoil (thickness 1.96%)

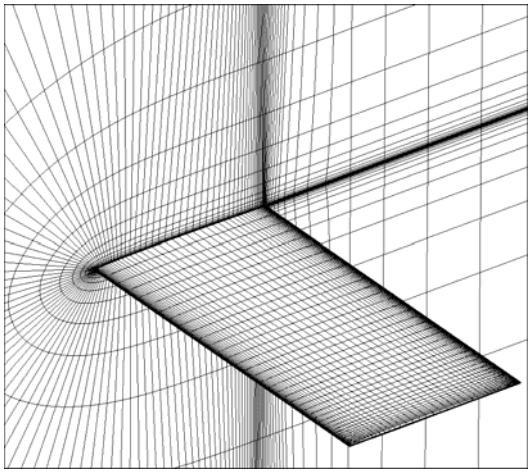

Fig.7 wing grid

5 Flapping Mode

Fig.8 is the sketch map of flapping motion. This is the preconcerted motion without deformation. In fact the wing will deform in flapping, and deformed wing will be shown latterly.

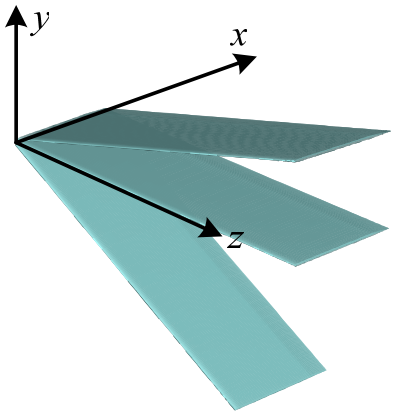

Fig.8 sketch map of flapping motion

The wing motion is only flapping. The flapping motion is defined as,

$$\psi(t) = \psi_{tip} \cos(\omega t) \qquad (9)$$

The reduced frequency is,

$$k = \frac{\omega c}{2U_\infty} \qquad (10)$$

Here, ψ_{tip} is the flapping angle, ω is the circle frequency, $\omega = 2\pi f$, f is flapping frequency, U_∞ is the freestream velocity, c is chord length.

6 Fluid-structure Coupling Method

Based on the section 3, the relationship between displacement and aerodynamic force is derived. A loosely-coupled method is chosen to solve the problem, and the fluid and structural solution communicate at the physical time-step level. At every time step, the aerodynamic force is calculated firstly, then the structure displacement is calculated by the force vector, and the force vector needs to be calculated again. When the structure deformation displacement and aerodynamic force are convergent, current time step is finished and next time step continues to be calculated.

The main scope of this paper is the deformation of flapping wing by the aerodynamic force. Although the aerodynamic force is unsteady, this still belongs to static aeroelastic problem for the inertia force is ignored.

The fluid-structure interaction flowchart is shown in Fig.9.

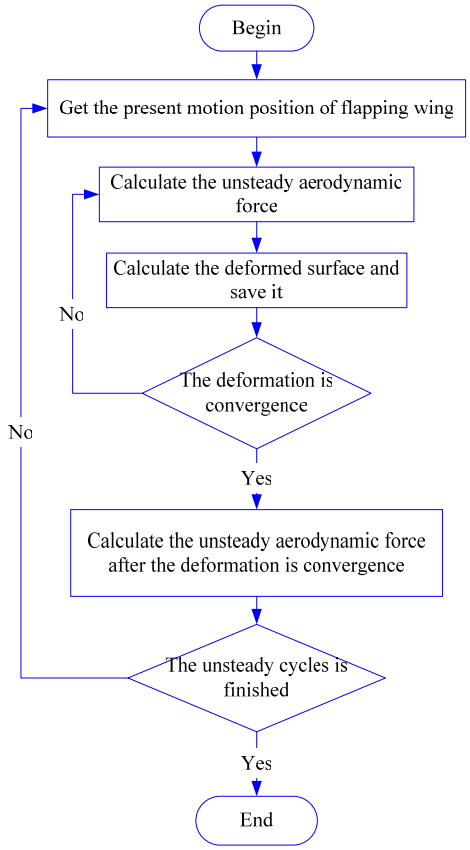

Fig.9 flowchart of fluid-structure coupling method

The relaxation parameter s is used to control the convergence process. Let D_i^* is the displacement of present step, D_{i-1} is the displacement of pre-step, then the present revised displacement is,

$$D_i = D_i^* + s(D_{i-1} - D_i^*), (0 < s < 1) \qquad (11)$$

After the displacement is convergent, $(D_{i-1} - D_i^*) \doteq 0$, also, $D_i \doteq D_i^*$, the effect of s is eliminated.

s can depress the fluctuation of displacement and make the calculation convergent more quickly. The parameter s doesn't change the final result, only change the convergence process.

The distributing surface forces are translated onto the structure nodes to calculate the structure deformation. The basic principle is to keep the force and moment balance and conserved.

7 Example

Numerical examples are calculated. The state parameters are: Ma=0.03, ψ_{tip}=25°, k=0.2, Re=7×10^4. This state is in the range of FMAV flight. The half aspect ratio of the wing is $A/2$=2.3. Three angles of attack are chosen: α_0=0, 5, 10° to research the aerodynamic principles.

Fig.10 is the lift coefficient results comparison between rigid wing and flexible wing.

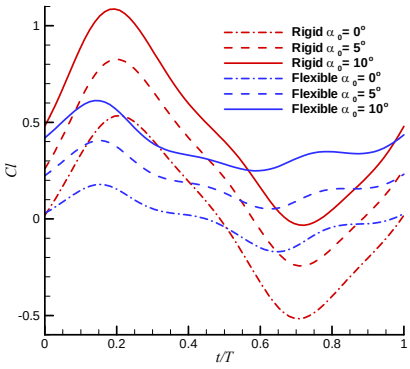

Fig.10 lift coefficient results comparison between rigid and flexible wings

Fig.10 shows that the lift generated by flexible flapping wing is less fluctuant than by rigid wing, which also means the flexible wing will fly more stably.

Fig.11 is the drag coefficient results comparison between rigid wing and flexible wing.

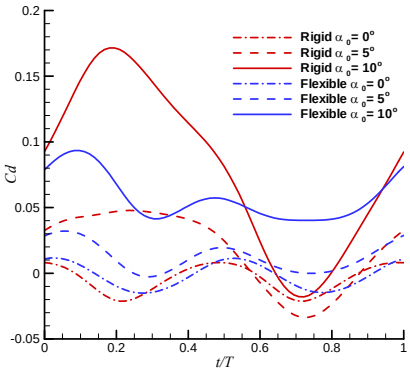

Fig.11 drag coefficient results comparison between rigid and flexible wings

Fig.11 shows that the drag generated by flexible flapping wing is also less fluctuant than by rigid wing, which is the same as lift coefficient.

Fig.12 is the average lift and drag coefficients comparison between rigid wing and flexible wing.

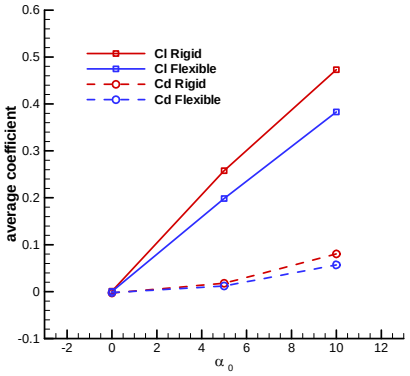

Fig. 12 average coefficients comparison between rigid and flexible wings

Fig.12 shows that the average lift and drag generated by flexible wing increase more slowly than rigid wing along with the increase of angle of attack. The results mean if a disturbance makes the angle of attack increase, the flexible flapping wing will generate less additional lift than rigid flapping wing, which makes the flight

of flexible flapping wing air vehicle more stable. The inbeing principle is the deformation of flexible wing weakens the aerodynamic force.

The drag generated by flexible wing is less than by rigid wing, which also means the thrust generated by flexible wing is more than by the rigid wing. The thrust of FMAV is generated only by flapping wing, which should be as big as possible.

Fig.13 is the wing deformation in the position of down stroke to the neutral position.

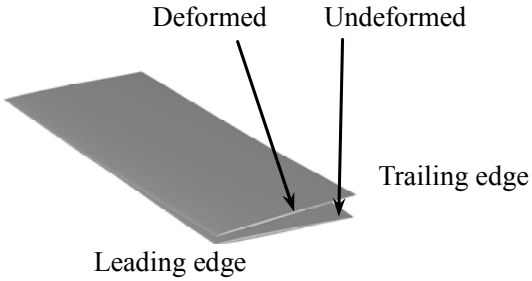

Fig.13 wing deformation in the position of down stroke to the neutral position in α_0=5°

The deformation way of flexible wing is caused by the structure stiffness. The leading edge deformation is less than the trailing edge because the stiffness of leading edge is more than the trailing edge. And the results of this paper are obtained based on this kind of structure. The analysis show the structure of flexible wing in this paper is successful to enhance the stability and increase the thrust.

8 Conclusion

The results show that the deformation of flexible wing can decrease the oscillating range of lift coefficient, and the average lift coefficient will decrease a little. The flexible wing can decrease the drag coefficient, that also means increasing the thrust coefficient because the deformation manner caused by the structure with stiffer leading edge. So the proper flexible wing is advantageous to flapping flight.

The method presented in this paper can be used to study the flexible flapping wing with light mass and elastic structure. This is a useful tool to analyze the true aerodynamic characteristics of micro flexible flapping wing.

References

[1] K D Jones, B M Castro, O Mahmoud, and M F Platzer. A numerical and experimental investigation of flapping-wing propulsion in ground effect [A]. AIAA 2002-0866.

[2] K D Jones, S J Duggan, and M F Platzer. Flapping-wing propulsion for a micro air vehicle [A]. AIAA 2001-0126.

[3] San-Yih Lin, and Jeu-Jiun Hu. Aerodynamic Performance Study of Flapping-Wing Flowfields [A]. AIAA 2005-4611.

[4] ZENG Rui, ANG Hai-song, MEI Yuan, JI Jian. Flexibility of Flapping Wing and Its Effect on Aerodynamic Characteristic [J]. Chinese Journal of Computational Mechanics. Vol.22, No.6, 2005, pp.750-754.

[5] XIE Hui, SONG Wen-ping, SONG Bi-feng. Numerical Solution of Navier-Stokes Equations for Flow over a Flapping Wing [J]. Journal of Northwestern Polytechnical University. Vol.26, No.1, 2008, pp.104-109.

[6] Yang Guowei, Qian Wei. Numerical Analyses of Transonic Flutter on an Aircraft [J]. Chinese Journal of Theoretical and Applied Mechanics. Vol.37, No.6, 2005, pp.769-776.

[7] Yin Xiangchao. Vibration theory and test technology [M]. Chinese mining university press. 2007, pp.45-54.

[8] HAN Zhong-hua, QIAO Zhi-de, XIONG Jun-tao. Development of an Efficient Viscous Preconditioning Method and Its Application to Numerical Simulation of Flows over Airfoils [J]. Journal of Northwestern Polytechnical University. pp 275-280.

[9] YANG Wen-qing, SONG Bi-feng, SONG Wen-ping. Distance Decreasing Method for Confirming Corresponding Cells of Overset Grids and Its Application[J]. Acta Aeronautica et Astronautica Sinica. Vol.30, No.2, 2009, pp.205-212.

[10] Alain Pelletier, Thomas J. Muller. Low Reynolds Number Aerodynamics of Low Aspect Ratio Wings. AIAA paper 99-3182.

Copyright Statement